Article

Design, Synthesis, and Characterizations of a Series of Pt Macrocycles and Fluorescent Sensing of Fe/Cu/Ni Through Metal Coordination

Sushobhan Ghosh, Rajesh Chakrabarty, and Partha Sarathi Mukherjee

Inorg. Chem., **2009**, 48 (2), 549-556 • DOI: 10.1021/ic801381p • Publication Date (Web): 11 December 2008

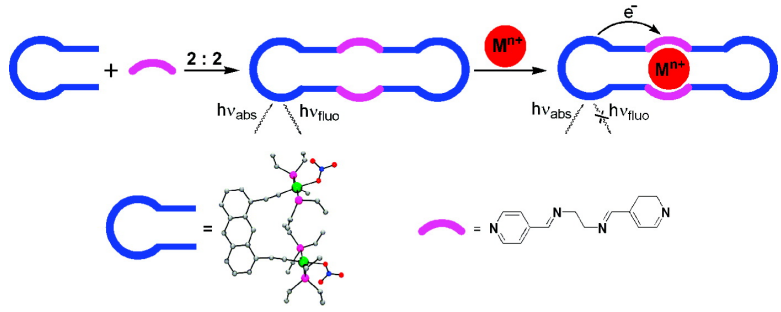

More About This Article

Additional resources and features associated with this article are available within the HTML version:

- Supporting Information
- Access to high resolution figures
- Links to articles and content related to this article
- Copyright permission to reproduce figures and/or text from this article

View the Full Text HTML

Inorg. Chem. **2009**, *48*, 549−556

Design, Synthesis, and Characterizations of a Series of Pt_4 Macrocycles and Fluorescent Sensing of $Fe^{3+}/Cu^{2+}/Ni^{2+}$ Through Metal Coordination

Sushobhan Ghosh, Rajesh Chakrabarty, and Partha Sarathi Mukherjee*

Department of Inorganic and Physical Chemistry, Indian Institute of Science, Bangalore 560 012, India

Received July 23, 2008

A Pt^{II}_2 organometallic "clip" (**1a**) containing ethynyl functionality is synthesized. Multinuclear NMR and electrospray ionization mass spectrometry characterized this "clip", and the molecular structure was determined in an X-ray single-crystal diffraction study. A series of discrete molecular rectangles (**2a**−**d**) have been synthesized from this "clip" in combination with dipyridyl-based linear linkers ($\mathbf{L_{1-4}}$) by a metal−ligand coordination driven self-assembly approach [where $\mathbf{L_1}$ = 4,4′-bipyridine, $\mathbf{L_2}$ = *trans*-1,2-bis(4-pyridyl)ethylene, $\mathbf{L_3}$ = N-(4-pyridyl)isonicotinamide, and $\mathbf{L_4}$ = N,N′-bis(4-pyridylidene)ethylenediamine]. Rectangle **2d** was designed using the imine-based ligand $\mathbf{L_4}$ to make it a system composed of a fluorophore−receptor−fluorophore combination. The imine N_4 pocket is the receptor site, while the anthracene-based "clip" is the fluorophore. Complex **2d** is fluorescent in nature and showed fluorescence quenching in solution upon the binding of hard transition metal ions (Fe^{3+}, Cu^{2+}, Ni^{2+}, and Mn^{2+}) into the N_4 pocket. The nonresponsive nature of the fluorescence intensity upon the addition of soft metal ions (Zn^{2+} and Cd^{2+}) having d^{10} configuration makes it a suitable sensor for transition metal ions. The fluorescence intensity of the Ni^{2+} bound complex was regained when the metal was removed by a stronger chelating 2,2′-dipyridyl ligand.

Introduction

The synthesis of supramolecular structures of finite shapes and sizes using the directional bonding approach has gained much attention since the discovery of the first supramolecular square in 1990.[1,2] The most important advantage of the coordination-driven self-assembly over the traditional covalent synthesis is that even very large molecules can be easily synthesized in fewer steps at a very high yield of the target product using appropriate building units.[3]

Rational design of structures of various shapes, sizes, and symmetries is the main feature of this method. Pd^{II} and Pt^{II} have long been among the favorite metal ions used for this purpose because of their rigid square-planar coordination environment. In a majority of cases, symmetrical polypyridyl ligands have been used with cis-protected metal centers to

* Author to whom correspondence should be addressed. Tel.: 91-80-2293-3352. Fax: 91-80-2360-1552. E-mail: psm@ipc.iisc.ernet.in.

(1) (a) Seidel, S. R.; Stang, P. J. *Acc. Chem. Res.* **2002**, *35*, 972. (b) Leininger, S.; Olenyuk, B.; Stang, P. J. *Chem. Rev.* **2000**, *100*, 853. (c) Holliday, B. J.; Mirkin, C. A. *Angew. Chem., Int. Ed.* **2001**, *40*, 2022. (d) Fiedler, D.; Leung, D. H.; Bergman, R. G.; Raymond, K. N. *Acc. Chem. Res.* **2005**, *38*, 351. (e) Kawano, M.; Fujita, M. *Coord. Chem. Rev.* **2007**, *251*, 2592. (f) Cooke, M. W.; Chartrand, D.; Hanan, G. S. *Coord. Chem. Rev.* **2008**, *252*, 903. (g) Cotton, F. A.; Lin, C.; Murillo, C. A. *Acc. Chem. Res.* **2001**, *34*, 759. (h) Amijs, C. H. M.; van Klink, G. P. M.; van Koten, G. *Dalton Trans.* **2006**, *308*. (i) Fujita, M.; Umemoto, K.; Yoshizawa, M.; Fujita, N.; Kusukawa, T.; Biradha, K. *Chem. Commun.* **2001**, *509*. (j) Rang, A.; Engeser, M.; Maier, N. M.; Nieger, M.; Lindner, W.; Schalley, C. A. *Chem.—Eur. J.* **2008**, *14*, 3855. (k) Hutin, M.; Schalley, C. A.; Bernardinelli, G.; Nitschke, J. R. *Chem.—Eur. J.* **2006**, *12*, 4069. (l) Schalley, C. A.; Baytekin, H. T.; Baytekin, B. *Macrocyclic Chemistry: Current Trends and Future*; Gloe, K., Ed.; Springer: Heidelberg, Germany, 2005; p 37. (m) Jeong, K. S.; Kim, S. Y.; Shin, U. S.; Kogej, M.; Hai, N. T. M.; Broekmann, P.; Jeong, N.; Kirchner, B.; Reiher, M.; Schalley, C. A. *J. Am. Chem. Soc.* **2005**, *127*, 17672.

(2) (a) Ghosh, S.; Mukherjee, P. S. *Organometallics* **2008**, *27*, 316. (b) Chi, K.-W.; Addicott, C.; Arif, A. M.; Das, N.; Stang, P. J. *J. Org. Chem.* **2003**, *68*, 9798. (c) Ghosh, S.; Mukherjee, P. S. *Organometallics* **2007**, *26*, 3362. (d) Ghosh, S.; Batten, S. R.; Turner, D. R.; Mukherjee, P. S. *Organometallics* **2007**, *26*, 3252. (e) Tabellion, F. M.; Seidel, S. R.; Arif, A. M.; Stang, P. J. *J. Am. Chem. Soc.* **2001**, *123*, 7740. (f) Tabellion, F. M.; Seidel, S. R.; Arif, A. M.; Stang, P. J. *J. Am. Chem. Soc.* **2001**, *123*, 11982. (g) Mukherjee, P. S.; Das, N.; Kryschenko, Y. K.; Arif, A. M.; Stang, P. J. *J. Am. Chem. Soc.* **2004**, *126*, 2464. (h) Das, N.; Mukherjee, P. S.; Arif, A. M.; Stang, P. J. *J. Am. Chem. Soc.* **2003**, *125*, 13950. (i) Splan, K. E.; Massari, A. M.; Morris, G. A.; Sun, S.-S.; Reina, E.; Nguyen, S. T.; Hupp, J. T. *Eur. J. Inorg. Chem.* **2003**, *2348*. (j) Santosh, G.; Ravikanth, M. *Inorg. Chim. Acta* **2005**, *358*, 2671. (k) Chang, S.-Y.; Um, M.-C.; Uh, H.; Jang, H.-Y.; Jeong, K.-S. *Chem. Commun.* **2003**, *2026*. (l) Whiteford, J. A.; Stang, P. J.; Huang, S. D. *Inorg. Chem.* **1998**, *37*, 5595. (m) Fujita, M.; Yazaki, J.; Ogura, K. *J. Am. Chem. Soc.* **1990**, *112*, 5645.

10.1021/ic801381p CCC: $40.75
Published on Web 12/11/2008

Scheme 1. Self-Assembly of Rectangles **2a**−**d**

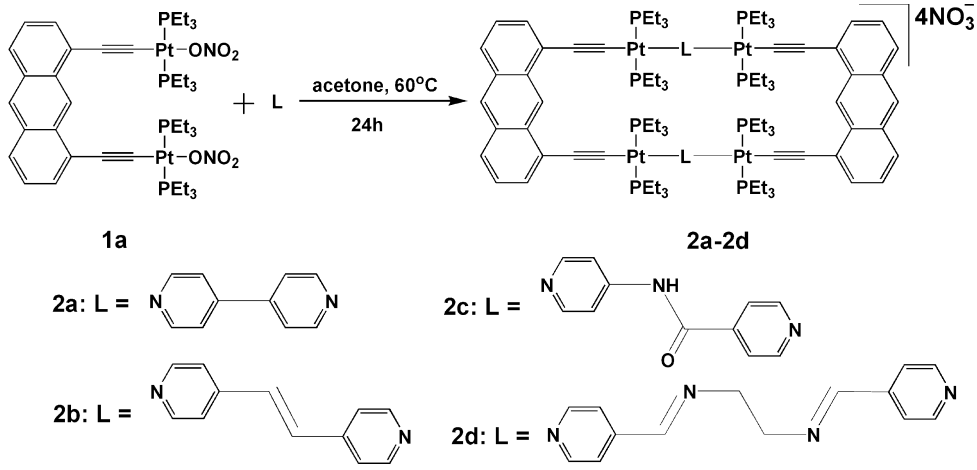

generate several 2D and 3D discrete assemblies.[2] Properties of a molecule are generally guided by the existing functional group(s). Thus, incorporation of the functional groups into assemblies may be an efficient way to guide the properties of the resulting architectures.[3a] Several functional groups[3]like porphyrin, calixarene, carborane, and acid-based receptors have been incorporated into self-assemblies.[4] Some of these architectures display interesting properties and have potential applications in various fields including host−guest chemistry, catalysis, and photo- and electrochemical sensing. In a recent communication, we have shown that incorporation of an ethynyl functionality into Pt-based nanoscopic architectures develops fluorescence behavior in the resulting assemblies and the possibility of using them as fluorescent sensors.[2a] Among the several 2D discrete assemblies, the rectangle is a relatively lesser known architecture since it is difficult to derive from the readily available cis-blocked metal acceptors. Stang's group established a novel approach of designing rectangles by the [2 + 2] self-assembly of a molecular "clip" and a linear linker.[3c,5] To extend Stang's methodology of designing rectangles using a "clip" as well as to introduce ethynyl functionality for fluorescent behavior, we have designed a new organometallic Pt^{II}_2 "clip" (**1a**) incorporating the ethynyl functionality (Scheme 1). A few luminescent supramolecules containing ethynyl functionality have been reported, of which rhenium-based molecular rectangles have dominated the literature.[6]

Here, we report the syntheses and characterizations of four new luminescent molecular rectangles (Scheme 1) of general formula $[\mathbf{1a}_2(\mu\text{-}\mathbf{L}_n)_2](NO_3)_4$ (**2a**−**d**) from the new molecular "clip" **1a** [for **2a**, $\mathbf{L_1}$ = 4,4′-bipyridine; **2b**, $\mathbf{L_2}$ = *trans*-1,2-bis(4-pyridyl)ethylene; **2c**, $\mathbf{L_3}$ = N-(4-pyridyl)isonicotinamide; **2d**, $\mathbf{L_4}$ = *N*,*N*′-bis(4-pyridylidene)ethylenediamine]. In the case of the rectangle **2d**, the presence of four imine nitrogen atoms inside the molecule makes it a suitable pocket for interaction with moderate hard 3d metal ions like Cu^{2+}, Ni^{2+}, Mn^{2+}, and so forth. The fluorescence of **2d** was quenched efficiently upon titration with metal ions Cu^{2+} and Ni^{2+}, indicating the possibility of a photoinduced electron transfer (PET) mechanism for the quenching.[7] The recovery of the luminescence by the addition of 2,2′-bipyridine that removes the 3d metal ions from the N_4-imine pocket shows immense potential application of this compound as a fluorescent switch tuned by metal ions. Interestingly, soft

(3) (a) Ghosh, S.; Mukherjee, P. S. *Org. Chem.* **2006**, *71*, 8412. (b) Ghosh, S.; Mukherjee, P. S. *Dalton Trans.* **2007**, *2542*. (c) Resendiz, M. J. E.; Noveron, J. C.; Disteldorf, H.; Fischer, S.; Stang, P. J. *Org. Lett.* **2004**, *6*, 651. (d) Olenyuk, B.; Levin, M. D.; Whiteford, J. A.; Shield, J. E.; Stang, P. J. *J. Am. Chem. Soc.* **1999**, *121*, 10434. (e) Tominaga, M.; Suzuki, K.; Murase, T.; Fujita, M. *J. Am. Chem. Soc.* **2005**, *127*, 11950. (f) Slone, R. V.; Benkstein, K. D.; Bélanger, S.; Hupp, J. T.; Guzei, I. A.; Rheingold, A. L. *Coord. Chem. Rev.* **1998**, *171*, 221. (g) Fan, J.; Whiteford, J. A.; Olenyuk, B.; Levin, M. D.; Stang, P. J.; Fleischer, E. B. *J. Am. Chem. Soc.* **1999**, *121*, 2741. (h) Das, N.; Ghosh, A.; Singh, O. M.; Stang, P. J. *Org. Lett.* **2006**, *8*, 1701. (i) Das, N.; Ghosh, A.; Arif, A. M.; Stang, P. J. *Inorg. Chem.* **2005**, *44*, 7130. (j) Mukherjee, P. S.; Min, K. S.; Arif, A. M.; Stang, P. J. *Inorg. Chem.* **2004**, *43*, 6345.

(4) (a) Dash, B. P.; Satapathy, R.; Maguire, J. A.; Hosmane, N. S. *Org. Lett.* **2008**, *10*, 2247. (b) Jude, H.; Disteldorf, H.; Fischer, S.; Wedge, T.; Hawkridge, A. M.; Arif, A. M.; Hawthorne, M. F.; Muddiman, D. C.; Stang, P. J. *J. Am. Chem. Soc.* **2005**, *127*, 12131. (c) Fujita, N.; Biradha, K.; Fujita, M.; Sakamoto, S.; Yamaguchi, K. *Angew. Chem., Int. Ed.* **2001**, *40*, 1718. (d) Fujita, N.; Biradha, K.; Fujita, M.; Sakamoto, S.; Yamaguchi, K. *Angew. Chem., Int. Ed.* **2001**, *40*, 1718. (e) Ikeda, A.; Ayabe, M.; Shinkai, S.; Sakamoto, S.; Yamaguchi, K. *Org. Lett.* **2000**, *2*, 3707. (f) Fan, J.; Whiteford, J. A.; Olenyuk, B.; Levin, M. D.; Stang, P. J. *J. Am. Chem. Soc.* **1999**, *121*, 2741. (g) Lee, S. J.; Mulfort, K. L.; Zuo, X.; Goshe, A. J.; Wesson, P. J.; Nguyen, S. T.; Hupp, J. T.; Tiede, D. M. *J. Am. Chem. Soc.* **2008**, *130*, 836. (h) Yamanoi, Y.; Sakamoto, Y.; Kusukawa, T.; Fujita, M.; Sakamoto, S.; Yamaguchi, K. *J. Am. Chem. Soc.* **2001**, *123*, 980. (i) Johannessen, S. C.; Brisbois, R. G. *J. Am. Chem. Soc.* **2001**, *123*, 3818.

(5) (a) Kuehl, C. J.; Mayne, C. L.; Arif, A. M.; Stang, P. J. *Org. Lett.* **2000**, *2*, 3727. (b) Kuehl, C. J.; Huang, S. D.; Stang, P. J. *J. Am. Chem. Soc.* **2001**, *123*, 9634.

(6) (a) Rajendran, T.; Manimaran, B.; Liao, R.-T.; Lin, R.-J.; Thanasekaran, P.; Lee, G.-H.; Peng, S.-M.; Liu, Y.-H.; Chang, I.-J.; Rajagopal, S.; Lu, K.-L. *Inorg. Chem. 42*, 6388. (b) Thanasekaran, P.; Liao, R.-T.; Liu, Y.-H.; Rajendran, T.; Rajagopal, S.; Lu, K.-L. *Coord. Chem. Rev.* **2005**, *249*, 1085. (c) Rajendran, T.; Manimaran, B.; Lee, F.-Y.; Lee, G.-H.; Peng, S.-M.; Wang, C. M.; Lu, K.-L. *Inorg. Chem.* **2000**, *39*, 2016.

(7) (a) Fabbrizzi, L.; Poggi, A. *Chem. Soc. Rev.* **1995**, 197−202 and references therein. (b) Fabbrizzi, L.; Licchelli, M.; Pallavicini, P.; Perotti, A.; Sacchi, D. *Angew. Chem., Int. Ed. Engl.* **1994**, *33*, 1975. (c) Woessner, S. M.; Helms, J. B.; Houlis, J. F.; Sullivan, B. P. *Inorg. Chem.* **1999**, *38*, 4380. (d) Chi, L.; Zhao, J.; James, T. D. *J. Org. Chem.* **2008**, *73*, 4684. (e) He, G.; Zhao, Y.; He, C.; Liu, Y.; Duan, C. *Inorg. Chem.* **2008**, *47*, 5169–5176. (f) Germain, M. E.; Knapp, M. J. *J. Am. Chem. Soc.* **2008**, *130*, 5422. (g) Souchon, V.; Leray, I.; Valeur, B. *Chem. Commun*, **2008**, *4224*. (h) Che, Y.; Yang, X.; Zang, L. *Chem. Commun.* **2008**, *1413*. (i) Frisch, M.; Cahill, C. L. *Dalton Trans.*, **2006**, *4679*.

Scheme 2. Possible Cyclic Products in the [4 + 2 + 2] Self-Assembly of a 90° Acceptor and Two Linear Linkers of Different Lengths

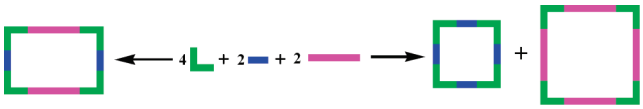

metal ions like Cd^{2+} and Zn^{2+} showed no such binding in the pocket, and thus no quenching of fluorescence intensity of **2d** was observed upon titration with these metal ions. This nonresponsive nature of the fluorescence intensity of **2d** upon titration with soft metal ions with d^{10} electronic configuration makes it a selective metal sensor for transition metal ions.

Results and Discussion

Design Principle, Synthesis, and Characterization of the "Clip" (1a). The first approach that will come to mind for designing a rectangle is the [4 + 2 + 2] self-assembly reaction of a 90° acceptor in combination with two linear linkers of different lengths. Only very few examples are known in the literature where rhenium-based rectangles have been prepared using this approach.[6] However, no success is known for Pt^{II} or Pd^{II} metals using this design principle. The main drawback of this approach is the nonselectivity in the formation of the desired rectangle because of the possibility of formation of a mixture of squares of different sizes from the combination of 90° corners with the individual linear linkers (Scheme 2).

Stang and co-workers have overcome this problem by employing a molecular "clip" in conjunction with a linear donor for the selective synthesis of [2 + 2] self-assembled macrocyclic rectangles.[5,2f,g] Recently, we have shown that incorporation of an ethynyl functionality into Pt-based discrete architectures can introduce fluorescent behavior and possible use as fluorescent sensors.[2a] To extend Stang's methodology of rectangle synthesis and to explore the possibility of designing fluorescent rectangles, we have prepared a molecular "clip" (**1a**) with the incorporation of an ethynyl functionality (Scheme 3).

1,8-Dichloroanthracene was reacted with (trimethylsilyl)acetylide magnesium bromide ($Me_3SiCCMgBr$), which was prepared by reacting ethylmagnesiumbromide with ethynyltrimethylsilane in THF under a nitrogen atmosphere. Hydrolysis of the resulting product, 1,8-bis(trimethylsilylethynyl)anthracene, in methanol using K_2CO_3 produced 1,8-diethynylanthracene. This 1,8-diethynylanthracene was then further reacted with 3.5 equiv of *trans*-$PtI_2(PEt_3)_2$ in the presence of CuI as a catalyst to give **1**, which was isolated (67%) in pure form by column chromatography. Then, **1** was treated with 2.1 equiv of $AgNO_3$ in a mixture of chloroform and methanol to obtain **1a** in 90% isolated yield.

The "clip" **1a** was fully characterized by NMR {^{1}H and ^{31}P}, as outlined in the Experimental Section (Supporting Information, Figures S1 and S2). Electrospray ionization (ESI) mass spectrometric analysis showed the expected peaks at m/z = 1149.2 and 543.4 due to M^+ and M^{2+}, respectively. Finally, the molecular structure of this new "clip" was unambiguously determined by X-ray single-crystal structure analysis. Suitable single crystals for X-ray diffraction were obtained by the slow diffusion of ether into the chloroform−methanol solution of **1a**. Figure 1 represents the ORTEP view of the molecular structure of the "clip" **1a**. The coordination geometry around each Pt^{II} is square-planar with a "P_2CO" environment. Crystallographic refinement parameters are assembled in Table 1, while Table 2 contains the selected bond lengths and angles. The intramolecular Pt−Pt distance was calculated to be 6.64 Å, which is slightly larger than the Pt−Pt distance in Stang's "clip".[5]

A significant feature regarding the structure of **1a** is that there is a slight dihedral twist ($\Phi = 15.3°$) between the two substituents at the 1 and 8 positions, which is likely due to the strong steric interaction between the PEt_3 units in the molecule. The two weakly bound nitrate anions coordinated to two Pt^{II} centers are almost parallel, which makes this molecule a molecular "clip".

Synthesis and Characterization of the Macrocycles 2a−d. The "clip" **1a** was treated with the linear donor ligands $\mathbf{L_{1-4}}$ [$\mathbf{L_1}$ for **2a**, 4,4′-bipyridine; $\mathbf{L_2}$ for **2b**, *trans*-1,2-bis(4-pyridyl)ethylene; $\mathbf{L_3}$ for **2c**, N-(4-pyridyl)isonicotinamide; $\mathbf{L_4}$ for **2d**, N,N′-bis(4-pyridylidene)ethylenediamine] in a 1:1 molar ratio in acetone to obtain the self-assemblies **2a−d** in high yields (Scheme 1).

The assemblies were characterized in solution by ^{1}H and ^{31}P NMR as well as by ESI mass spectrometry. The product formations were clearly indicated from the ^{31}P NMR spectra. In the case of **1a**, the ^{31}P NMR showed a single peak at 19.06 ppm, which is upfield-shifted to 14.26, 14.33, 14.98, and 13.91 ppm for **2a**, **2b**, **2c**, and **2d**, respectively, with the appearance of concomitant platinum satellites. The upfield shifts of the phosphorus peak indicated the ligand-to-Pt electron donation and thus the metal−ligand coordination. In the case of **2c**, the two peaks in ^{31}P NMR are due to the nonsymmetrical nature of the donor amide ligand, where one of the pyridyl groups is connected to −NH while the other is connected to C═O. ^{1}H NMR spectra also showed a downfield shift of the pyridyl protons as expected due to the coordination to the metal center (Figure 2 and Supporting Information, Figure S3−S9).

In the case of **2c**, the formation of two different linkage isomers is possible due to the different connectivity of the nonsymmetrical bridging amide linker (Scheme 4). ^{31}P NMR in both the isomers should show two peaks, and thus phosphorus NMR cannot conclude which isomer has formed. Interestingly, ^{1}H NMR showed a single sharp peak due to the H_1 of anthracene, which indicated the formation of isomer **2c**, since H_1 protons in the alternative isomer (**2c′**) are nonequivalent (Scheme 4). In a previous report, we showed the selective formation of a single isomer using the same amide ligand using a different Pt_2 acceptor.[3b]

The formation of [2 + 2] self-assembled macrocycles (**2a−d**) was finally proven by ESI-MS spectrometric analysis, where multiply charged molecular ions corresponding to the macrocycles were observed. The ESI-MS experiments were performed in a methanol solution of the corresponding macrocycles. The multiply charged molecular ions for **2a** at m/z = 1305.93, 1187.13, and 622.07 are ascribed to the

Scheme 3. Synthesis of the Molecular "Clip" **1a** (Path B) and Stang's "Clip" (Path A)

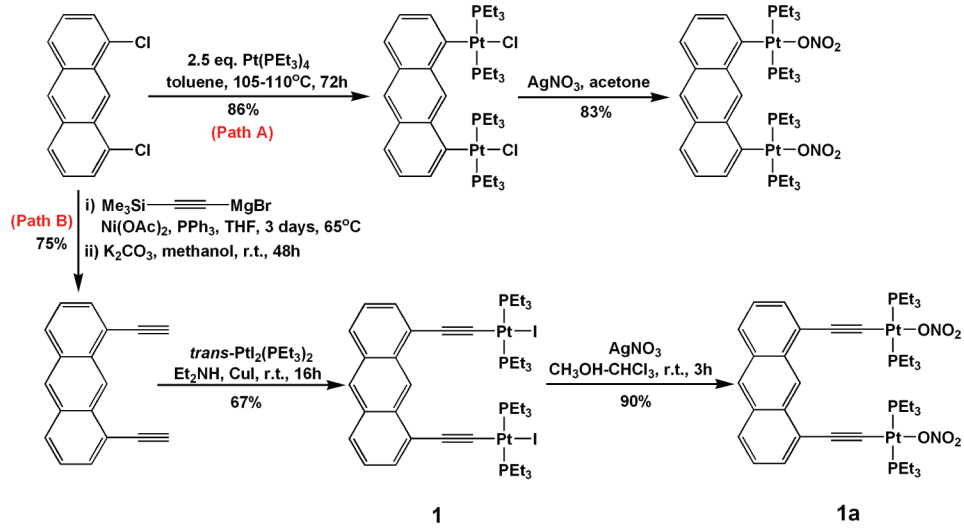

Table 1. Crystallographic Data and Structure Refinement Parameters for **1a**

formula	$C_{42}H_{68}N_2O_6P_4Pt_2$
M	1211.04
T/K	150
λ/Å	0.71073
cryst syst	monoclinic
space group	*C*2/*c*
a/Å	14.239 (16)
b/Å	12.934 (16)
c/Å	27. 953 (4)
α/deg	90.0
β/deg	104.426 (4)
γ/deg	90.0
V/Å^3	4985.8 (11)
Z	4
ρ_{calcd}/g cm^{-3}	1.613
μ/mm^{-1}	5.776
F (000)	2392
collected reflns	17738
unique reflns	4403
GOF on F^2	1.135
$R_1{}^a$ [$I > 2\sigma(I)$]	0.0895
wR_2	0.1806

^{a} $R = \sum ||F_o| - |F_c||/\sum |F_o|$. $R_w = [\sum\{w(F_o^2 - F_c^2)^2\}/\sum\{w(F_o^2)^2\}]^{1/2}$.

cations $[\mathbf{2a}-2NO_3^-]^{2+}$, $[(\mathbf{2a}-2NO_3^--2PEt_3)]^{2+}$, and $[\mathbf{2a}-4NO_3^-]^{4+}$; for **2b** at *m*/*z* = 1332.20, 1213.53, 867.13, and 634.73 are ascribed to the cations $[\mathbf{2b}-2NO_3^-]^{2+}$, $[\mathbf{2b}-2NO_3^--2PEt_3]^{2+}$, $[\mathbf{2b}-3NO_3^-]^{3+}$, and $[\mathbf{2b}-4NO_3^-]^{4+}$; for **2c** at *m*/*z* = 1349.12 and 878.21 are ascribed to $[\mathbf{2c}-2NO_3^-]^{2+}$ and $[\mathbf{2c}-3NO_3^-]^{3+}$; and for **2d** peaks at *m*/*z* = 1387.00, 1269.14, 905.00, and 786.20 are ascribed to $[\mathbf{2d}-2NO_3^-]^{2+}$, $[\mathbf{2d}-2NO_3^--2PEt_3]^{2+}$, $[\mathbf{2d}-3NO_3^-]^{3+}$, and $[\mathbf{2d}-3NO_3^--3PEt_3]^{3+}$, respectively. The isotropic distribution of one peak confirmed the charged state (Figure 3 and Supporting Information, Figures S10−S11).

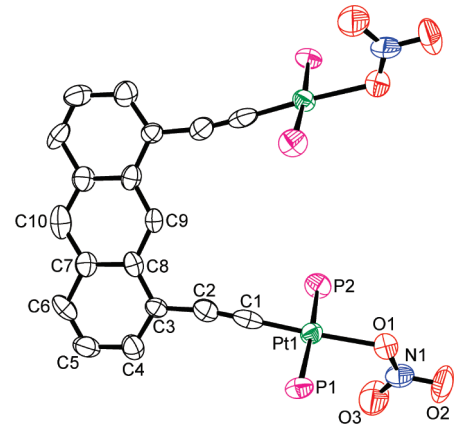

Figure 1. Labeled ORTEP (30% probability) representation of the "clip" **1a**. Ethyl groups of the PEt_3 and hydrogen atoms are omitted for clarity.

Several attempts to grow single crystals for the complexes were unsuccessful. Geometry optimization for compound **2a** done using the MM2 force field method showed the optimized structure to be a rectangle, as expected (Supporting Information, Figure S12).

UV−Visible Absorption Studies. The electronic absorption spectrum of compound **2d** in methanol (Figure 4) shows strong absorption bands at 424 nm (ε = 27 244 M^{-1} cm^{-1}), 400 nm (ε = 27 355 M^{-1} cm^{-1}), 380 nm (ε = 12 658 M^{-1} cm^{-1}), 353 nm (ε = 12 266 M^{-1} cm^{-1}), and 258 nm (ε = 13 3176 M^{-1} cm^{-1}). The peak at 258 nm is tentatively assigned to an intraligand $\pi \rightarrow \pi^*$ transition [$\pi \rightarrow \pi^*$ (C≡C−An)]. The peaks corresponding to **2a**, **2b**, and **2c** are similar to those for complex **2d.**

Fluorescent Studies. Fluorescence enhancement or quenching can be used as an efficient tool for the selective detection of ions or other chemical entities in solution. Discovery of fluorescent sensors for the selective detection of chemicals and ions has been a very active field of current research. Recently, we developed a Pt−ethynyl-based fluorescent sensor for the detection of nitroaromatics, which are the chemical signatures of many explosives.[2a] A fluorescent sensor is basically a two-component system, in which a light-emitting group is covalently linked to a receptor specific for a particular ion or substrate.[8,9] Sensor efficiency requires that

(8) (a) Kumar, A.; Ali, A.; Rao, C. P. *J. Photochem. Photobiol. A* **2006**, *177*, 164. (b) Kim, J. S.; Shon, O. J.; Rim, J. A.; Kim, S. K.; Yoon, J. *J. Org. Chem.* **2002**, *67*, 2348. (c) Matsumoto, H.; Shinkai, S. *Tetrahedron Lett.* **1996**, *37*, 77.

(9) (a) Bissell, R. A.; de Silva, A. P.; Gunaratne, H. Q. N.; Lynch, P. L. M.; Maguire, G. E. M.; Sandanayake, K. R. A. S. *Chem. Soc. Rev.* **1992**, *187*. (b) Gubelmann, M.; Harriman, A.; Lehn, J.-M.; Sessler, J. L. *J. Chem. Soc., Chem. Commun.* **1988**, *77*. (c) Patra, G. K.; Golding, I. *J. Chem. Soc., Dalton Trans.* **2002**, *1051*.

Table 2. Selected Bond Distances (Å) and Angles (deg) of **1a**

P1(1)−C(1)	1.860(3)	P1(1)−O(1)	2.140(15)	Pt(1)−P(2)	2. 297(5)
Pt(1)−P(1)	2.315(5)	O(1)−N(1)	1.220(2)	O(2)−N(1)	1.240(2)
O(3)−N(1)	1.210(2)	C(2)−C(1)	1.250(3)	C(2)−C(3)	1.460(3)
C(3)−C(4)	1.370(2)	C(3)−C(8)	1.420(2)	C(8)−C(9)	1.410(2)
C(1)−Pt(1)−O(1)	176.7(8)			C(1)−Pt(1)−P(2)	87.60(6)
P(2)−Pt(1)−O(1)	92.50(4)			C(1)−Pt(1)−P(1)	89.20(6)
P(1)−Pt(1)−O(1)	90.80(4)			P(1)−Pt(1)−P(2)	175.4(2)
N(1)−O(1)−Pt(1)	116.8(16)			O(3)−N(1)−O(2)	120.0(2)
C(2)−C(1)−Pt(1)	175.0(2)			C(1)−C(2)−C(3)	171.0(2)

Scheme 4. Two Possible Macrocyclic Linkage Isomers for the [2 +2] Self-Assembly of **1a** and L_3

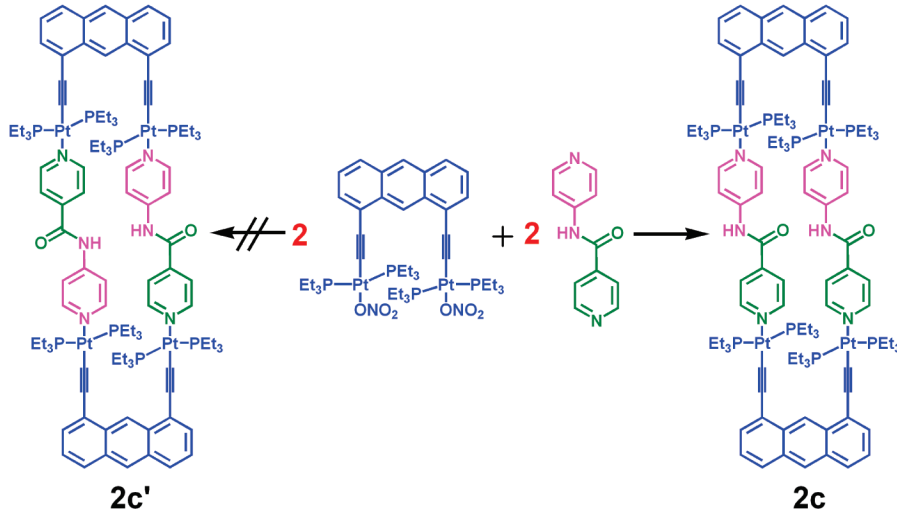

the ion-receptor interaction modify the fluorescence of the light-emitting unit. Hence, the fluorescence can be switched on and off, depending on the nature of ion/substrate−receptor interaction.[10] Because of its strong luminescence and chemical stability, the anthracene unit has been widely used in the design of fluorescent sensors. It has also been well established that Pt−ethynyl compounds show luminescence behavior.[11] Keeping these two facts in mind, we have designed the rectangle **2d** with a N_4 receptor site for binding suitable metal ions.

Complexes **2a**−**d** show an emission band at around 460 nm upon excitation at 400 nm in a methanol solution (Figure 5). Our designed rectangle **2d** has an anthracene-based fluorophore required for a fluorescent sensor and a N_4 pocket containing four imine nitrogen atoms inside the molecule which can coordinate to the metal ions of appropriate size.

The fluorescence intensity of this compound is gradually quenched when titrated with Mn^{2+}, Fe^{3+}, Ni^{2+}, and Cu^{2+} ions (Figure 6 and Supporting Information). In the case of Fe^{3+}, a 10^{-5} M solution of the metal ion was enough to show efficient fluorescent quenching of **2d**. Interestingly, metal ions having a completely filled d orbital. For example, Zn^{2+} or Cd^{2+} do not quench the fluorescence intensity of **2d**. The fluorescence intensity of the Ni^{2+} bound rectangle **2d** increased when titrated with a stronger chelating 2,2′-bipyridine ligand (Supporting Information).

This observation can be explained by the PET mechanism, which goes via excited-state electron transfer (Scheme 5).[12] The rectangle can be considered as an ideal combination of fluorophore−receptor−fluorophore, where the organometallic "clip" units are the fluorophores and the imine N_4 pocket is the receptor. The 3d series transition metal ions having incompletely filled d orbitals can drag the electron after excitation and can go to lower oxidation state(s). On the other hand, in the case of the Zn^{2+} ion, the nonavailability of the variable oxidation states as well as the fact that it has a stable d^{10} electronic configuration, it does not consume the electron. Hence, PET does not occur, and the fluorescence of **2d** is not quenched in the presence of Zn^{2+}. This nonresponsive nature of Zn^{2+} in the fluorescence quenching may also be due to the soft-acid character of Zn^{2+}, which is not suitable to bind in the hard donor N_4 pocket. Moreover, when 2,2′-

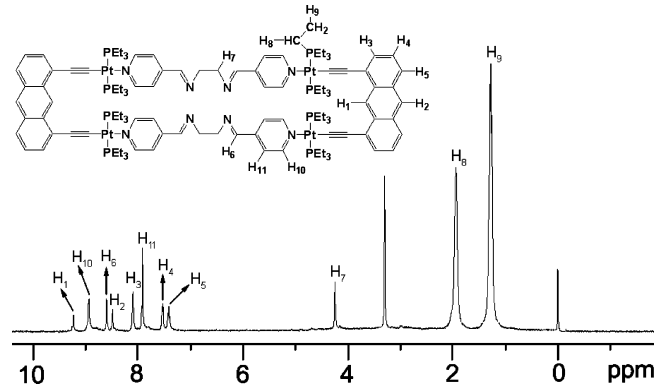

Figure 2. ^{1}H NMR (400 MHz) spectrum of **2d** in CD_3OD with the peak assignments.

(10) Goulle, V.; Harriman, A.; Lehn, J.-M. *J. Chem. Soc., Chem. Commun.* **1993**, *1034*.

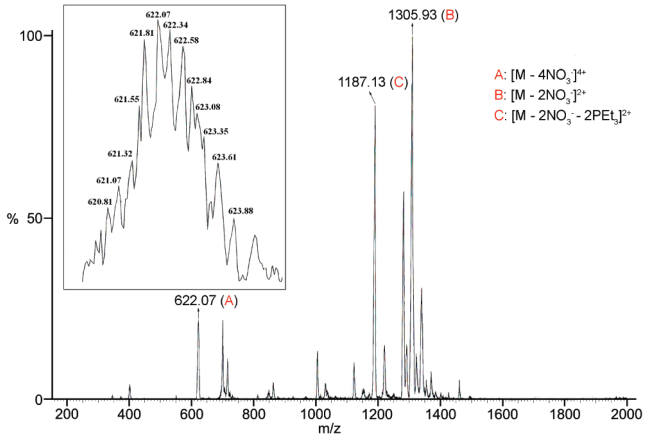

Figure 3. ESI-MS spectrum of complex **2a** in MeOH solution. Inset: Experimental isotropic distribution pattern for the peak at $[M - 4NO_3^-]^{4+}$.

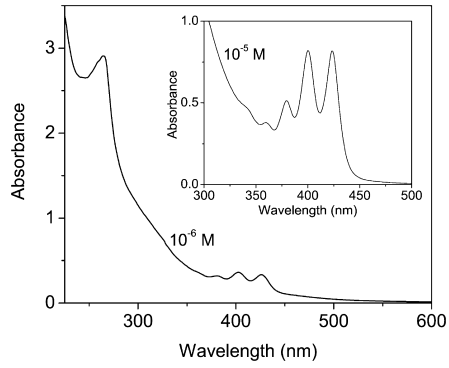

Figure 4. Electronic spectral absorptions for **2d** in methanol based on the measurements in 3×10^{-6} M and 3×10^{-5} M (inset) solutions.

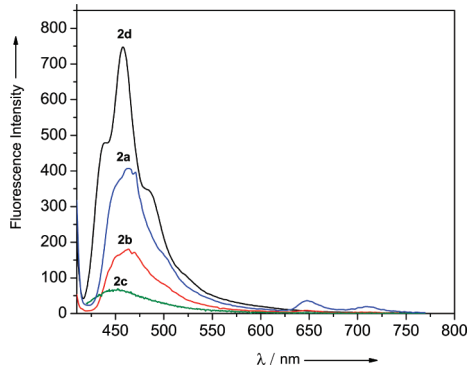

Figure 5. Emission spectra of complexes **2a**−**2d** in methanol (3×10^{-5} M).

bipyridine is added to the solution of [**2d** + Ni^{2+}], the fluorescence intensity gradually increases. 2,2′-Bipyridine is a stronger chelating ligand, and it removes the Ni^{2+} ion from the N_4 pocket of **2d**. PET stops, and thus the fluorescence intensity is regained. This introduces a new prospect of using Cu^{2+} and Ni^{2+} ions as tunable parameters for the change of one physical property of the molecule, and hence these ions can be used as switchable systems for **2d**.

Conclusion

In conclusion, we have synthesized and characterized a series of discrete molecular rectangles (**2a**−**d**) via directional self-assembly of a new organometallic Pt^{II}_2 molecular "clip" (**1a**) as the acceptor and dipyridyl donor linear linkers (**L**$_{1-4}$). In continuation of our recent communication,[2c] we have introduced a Pt−ethynyl functionality to design the "clip" **1a**. The rectangle **2d** is a system composed of a fluorophore−receptor−fluorophore combination, which is required for a fluorescent sensor. An anthracene-based "clip" acceptor has been used as the fluorophore, while the imine-based donor was specially designed in a way to develop a N_4 pocket in the center of the rectangle. The imine N_4 moiety is known to be suitable for moderate hard transition metal ions. All four rectangles showed fluorescent behavior. Due to having a metal ion receptor site in **2d**, solution fluorescence intensity was quenched efficiently upon titration with 3d transition metal ions like Mn^{2+}, Fe^{3+}, Ni^{2+}, and Cu^{2+}. Interestingly, no such quenching was observed when titration was performed with soft metal ions (Zn^{2+} or Cd^{2+}) containing a d^{10} electronic configuration. The quenching of the fluorescence intensity of **2d** by transition metal ions was explained qualitatively by the PET mechanism. Precise design of this rectangle and the presence of a specific binding core for metal ions make it a suitable fluorescent sensor for transition metal ions. Stang and co-workers have recently reported a supramolecular self-assembled optical sensor discovered in UV studies for Ni^{2+} and Cd^{2+}.[3c] However, the present rectangle **2d** represents a unique fluorescent sensor for the detection of transition metal ions. While there is enough room for improvement in the response of this kind of supramolecule toward other substrates, the Pt backbone with anthracene and ethynyl functionalities in conjugation provides an excellent starting material for new chemical sensors. The use of a specially designed shape-selective metal-based linker and the preparation of functional assemblies has the potential to considerably expand the range of the directional bonding paradigm in self-assembly.

Experimental Section

Materials and Methods. All solvents were dried and distilled according to standard literature procedures. 4,4′-Bipyridine, *trans*-1,2-bis(4-pyridyl)ethylene, pyridine-4-aldehyde, isonicotinylchloride hydrochloride, and 4-aminopyridine were purchased from Aldrich (U. S. A.) and were used without further purification. K_2PtCl_4 was purchased from Arora Matthey (India). N-(4-Pyridyl)isonicotinamide,[13] N,N′-bis(4-pyridylidene)ethylenediamine,[14] and 1,8-diethynylanthracene[15] were prepared following the reported procedures. Fluorescence studies were carried out on a Perkin-Elmer LS50B luminescence spectrometer. Absorption studies were carried out on a Perkin-Elmer LAMBDA 35 UV visible spectrophotometer. NMR spectra were recorded using a BRUKER 400 MHz machine.

(11) (a) Zhang, L.; Niu, Y.-H.; Jen, A. K.-Y.; Lin, W. *Chem. Commun.* **2005**, *1002*. (b) Jiang, H.; Lin, W. *J. Am. Chem. Soc.* **2003**, *125*, 8084. (c) Hu, J.; Lin, R.; Yip, J. H. K.; Wong, K.-Y.; Ma, D.-L.; Vittal, J. J. *Organometallics* **2007**, *26*, 6533.
(12) (a) Ikeda, A.; Udzu, H.; Zhong, Z.; Shinkai, S.; Sakamoto, S.; Yamaguchi, K. *J. Am. Chem. Soc.* **2001**, *123*, 3872. (b) Schnebeck, R.-D.; Randaccio, L.; Zangrando, E.; Lippert, B. *Angew. Chem., Int. Ed.* **1998**, *37*, 119.
(13) Kumar, D. K.; Jose, D. A.; Dastidar, P.; Das, A. *Langmuir* **2004**, *20*, 10413.
(14) Sun, W.-Y.; Fei, B.-L.; Okamura, T.-A.; Tang, W.-X.; Ueyama, N. *Eur. J. Inorg. Chem.* **2001**, *1855*.
(15) Pauvert, M.; Laine, P.; Jonas, M.; Weist, O. *J. Org. Chem.* **2004**, *69*, 543.

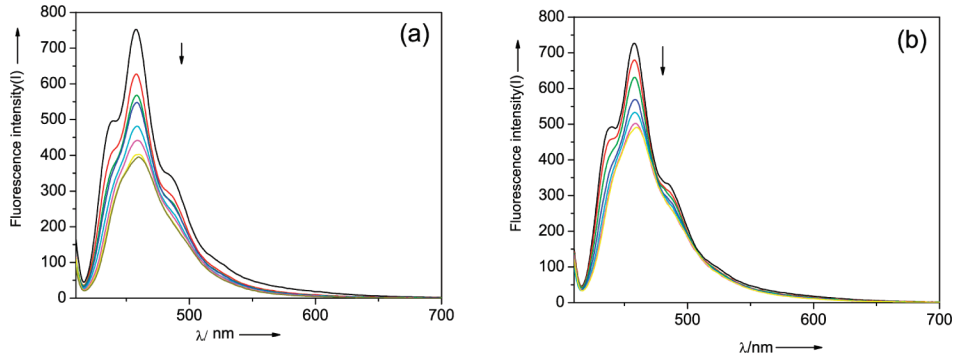

Figure 6. Quenching of fluorescence intensity of **2d** (3×10^{-5} M in methanol) by the gradual addition of (a) Cu^{2+}, 7.33×10^{-4} M to 6.39×10^{-3} M, and (b) Ni^{2+}, 6.31×10^{-4} M to 2.77×10^{-3} M.

Scheme 5. Mechanism of Action of a Molecular Switch

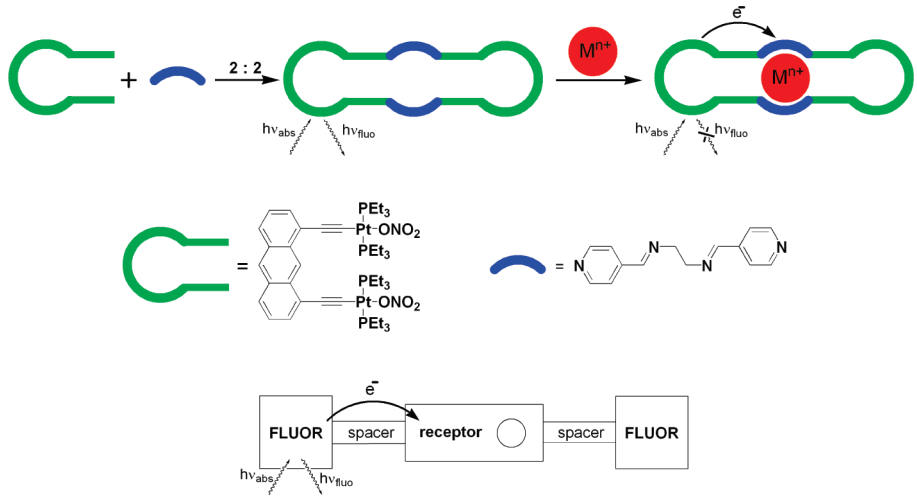

X-Ray Crystallographic Data Collection and Refinement. The crystal data for the "clip" **1a** were collected on a Bruker SMART APEX CCD diffractometer using the SMART/SAINT software.[16] X-ray-quality crystals were mounted on a glass fiber with traces of viscous oil. Intensity data were collected using graphite-monochromatized Mo Kα radiation (0.71073 Å) at 150 K. The structure was solved by direct methods using the SHELX-97[17] program incorporated into WinGX.[18] Empirical absorption corrections were applied with SADABS.[19] All non-hydrogen atoms were refined with anisotropic displacement coefficients. Hydrogen atoms were assigned isotropic displacement coefficients, $U(H) = 1.2U(C)$ or $1.5U$(C-methyl), and their coordinates were allowed to ride on their respective carbons. Structures were drawn using ORTEP-3 for Windows.[20]

Synthesis of the Organometallic Acceptor "Clip"1a. To a 100 mL round-bottom Schlenk flask were added *trans*-$PtI_2(PEt_3)_2$ (1198.8 mg, 1.75 mmol) and 1,8-diethynylanthracene (113.0 mg, 0.5 mmol), and the flask was put under a vacuum. Then, nitrogen was purged into the flask. A total of 20 mL of dry and degassed toluene and 10 mL of dry and deoxygenated diethylamine were added. The solution was stirred for 10 min at room temperature before 20.0 mg of CuI was added in one portion under nitrogen. After 2 h at room temperature, a greenish yellow fluorescent precipitate started to appear. The solvent was removed under a vacuum after 16 h of stirring at room temperature. The resulting greenish yellow residue was separated by column chromatography on silica gel with a solvent mixture (2:1 benzene/hexane). The "clip" **1** was isolated in 67% yield. Anal. calcd. (found) for $C_{42}H_{68}I_2P_4Pt_2$: C, 37.62 (37.59); H, 5.11 (5.23). ^{1}H NMR ($CDCl_3$, 400 MHz): δ 9.43 (s, 1H), 8.37 (s, 1H), 7.83 (d, 2H), 7.49 (d, 2H), 7.34 (d, 2H), 2.26 (q, 24H), 1.18 (t, 36H). ^{31}P NMR ($CDCl_3$): δ 8.35 (s, $^1J_{Pt-P}$ = 2756 Hz).

To a stirred solution of silver nitrate (25.1 mg, 0.15 mmol) in methanol was added a solution of **1** (100.0 mg, 0.07 mmol) in chloroform. Immediately, a yellowish white precipitate appeared. After stirring for 3 h, this precipitate was filtered through Celite, and the clear solution was evaporated to get **1a** in 90% yield. Anal. calcd (found) for $C_{42}H_{68}N_2O_6P_4Pt_2$: C, 41.65 (41.32); H, 5.66 (5.51); N, 2.31 (2.19). ^{1}H NMR ($CDCl_3$, 400 MHz): δ 9.27 (s, 1H), 8.35 (s, 1H), 7.82 (d, 2H), 7.42 (d, 2H), 7.35 (d, m), 2.00 (q, 24H), 1.27 (t, 36H). ^{13}C NMR ($CDCl_3$): δ 132.1 (2C, anthracene), 131.8 (2C, anthracene), 130.7 (2C, anthracene), 127.6 (2C, anthracene), 126.5 (2C, anthracene), 126.3 (2C, anthracene), 125.4 (2C, anthracene), 124.1 (2C, ethynyl), 103.3 (2C, ethynyl), 15.1 (12C, PEt_3), 8.1 (12C, PEt_3). ^{31}P NMR ($CDCl_3$): 19.06 (s, $^1J_{Pt-P}$ = 3072 Hz).

General Synthetic Procedure for 2a−d. To the stirred slurry of **1a** in acetone at 60 °C was added a solution of the corresponding ligand ($\mathbf{L_{1-4}}$) in acetone in a 1:1 ratio. Initially, a clear solution was formed, which upon further stirring overnight yielded a light

(16) *SMART/SAINT*; Bruker AXS, Inc.: Madison, WI, 2004.
(17) Sheldrick, G. M. *SHELX-97*; University of Göttingen: Göttingen, Germany, 1998.
(18) Farrugia, L. J. *J. Appl. Crystallogr.* **1999**, *32*, 837. Farrugia, L. J. *WinGX*, version 1.65.04; Department of Chemistry, University of Glasgow: Glasgow, Scotland, 2003.
(19) Sheldrick, G. M. *SADABS*; University of Göttingen, Göttingen, Germany, 1999.
(20) ORTEP-3 for Windows, version 1.08: Farrugia, L. J. *J. Appl. Crystallogr.* **1997**, *30*, 565.

yellow precipitate. The solid product was washed several times with diethylether and dried under a vacuum.

2a. Complex **1a** (12.1 mg, 0.01 mmol) and 4,4′-bipyridine (**L_1**; 1.6 mg, 0.01 mmol) were reacted in acetone to obtain **2a** in 96% yield. Anal. calcd (found) for $C_{104}H_{152}N_8O_{12}P_8Pt_4$: C, 45.68 (45.47); H, 5.60 (5.84); N, 4.09 (3.94). ESI-MS (*m*/*z*): 1305.93 [**2a** − $2NO_3^-$]$^{2+}$, 1187.13 [(**2a** − $2NO_3^-$ − $2PEt_3$)]$^{2+}$, 622.07 [**2a** − $4NO_3^-$]$^{4+}$. IR data (KBr pellet, ν_{max}/cm^{-1}) for **2a**: 2105 (C≡C). ^{1}H NMR ($CDCl_3$, 400 MHz): δ 9.29 (s, 2H, anthracene-H), 9.1 (d, 8H, pyridine-H), 8.6 (d, 8H, pyridine-H), 8.4 (s, 2H, anthracene-H), 7.88 (d, 4H, anthracene-H), 7.5 (d, 4H, anthracene-H), 7.2 (d, 4H, anthracene-H), 1.79 (q, 48H, $-CH_2$), 0.9 (t, 72H, $-CH_3$). ^{13}C NMR (CH_3NO_2 + CD_3OD): δ 154.0 (16C, **L_1**), 132.2 (8C, anthracene), 131.5 (4C, anthracene), 127.2 (4C, anthracene), 126.2 (8C, anthracene), 125.6 (4C, anthracene), 122.7 (4C, ethynyl), 122.1 (4C, **L_1**), 87.1 (4C, ethynyl), 14.6 (24C, PEt_3), 7.7 (24C, PEt_3). ^{31}P NMR ($CDCl_3$): δ 14.26 (s, $^1J_{Pt-P}$ = 2888 Hz).

2b. Complex **1a** (12.1 mg, 0.01 mmol) and *trans*-1,2-bis(4-pyridyl)ethylene (**L_2**; 1.8 mg, 0.01 mmol) were reacted in acetone to obtain **2b** in 90% yield. Anal. calcd (found) for $C_{108}H_{156}N_8O_{12}P_8Pt_4$: C, 46.55 (46.32); H, 5.64 (5.73); N, 4.02 (4.00). ESI-MS (*m*/*z*): 1332.20 [**2b** − $2NO_3^-$]$^{2+}$, 1213.53 [**2b** − $2NO_3^-$ − $2PEt_3$]$^{2+}$, 867.13 [**2b** − $3NO_3^-$]$^{3+}$, 634.73 [**2b** − $4NO_3^-$]$^{4+}$. IR data (KBr pellet, ν_{max}/cm^{-1}) for **2b**: 2105 (C≡C), 1611 (C═C). ^{1}H NMR ($CDCl_3$, 400 MHz): δ 9.2 (s, 2H, anthracene-H), 8.9 (d, 8H, pyridine-H), 8.39 (s, 2H, anthracene-H), 8.2 (d, 8H, pyridine-H), 7.85 (d, 4H, anthracene-H), 7.5 (d, 4H, anthracene-H), 7.39 (d, 4H, anthracene-H), 7.18 (s, 4H, C═CH), 1.8 (q, 48H, $-CH_2$), 1.1 (t, 72H, $-CH_3$). ^{13}C NMR (CH_3NO_2 + $CDCl_3$): δ 154.2 (8C, **L_2**), 150.1 (8C, **L_2**), 133.4 (8C, anthracene), 132.8 (4C, anthracene), 126.9 (8C, anthracene), 123.5 (4C, anthracene), 123.0 (4C, anthracene), 119.1 (4C, ethynyl), 118.2 (4C, **L_2**), 106.1 (4C, **L_2**), 87.2 (4C, ethynyl), 15.9 (24C, PEt_3), 9.0 (24C, PEt_3). ^{31}P NMR ($CDCl_3$): δ 14.5 (s, $^1J_{Pt-P}$ = 2960 Hz).

2c. Complex **1a** (12.1 mg, 0.01 mmol) and N-(4-pyridyl)isonicotinamide (**L_3**; 2.0 mg, 0.01 mmol) were reacted in acetone to obtain **2c** in 95% yield. Anal. calcd (found) for $C_{106}H_{158}N_{10}O_{14}P_8Pt_4$: C, 45.07 (44.83); H, 5.63 (5.62); N, 4.96 (4.74). ESI-MS (*m*/*z*): 1349.12 [**2c** − $2NO_3^-$]$^{2+}$, 878.21 [**2c** − $3NO_3^-$]$^{3+}$. IR data (KBr pellet, ν_{max}/cm^{-1}) for **2a**: 2105 (C≡C), 1696 (C═O). ^{1}H NMR ($CDCl_3$, 400 MHz): δ 12.05 (s, 2H, NH), 9.2 (s, 2H, anthracene-H), 8.95 (d, 4H, pyridine-H), 8.46 (s, 2H, anthracene-H), 8.41−8.32 (m, 8H, pyridine-H), 7.92 (d, 4H, anthracene-H), 7.59 (m, 4H, anthracene-H), 7.43 (m, 4H, anthracene-H), 7.34 (d, 4H, pyridine-H), 1.95 (q, 48H, $-CH_2$), 1.3 (t, 72H, $-CH_3$). ^{13}C NMR (CH_3NO_2 + $CDCl_3$): δ 170.1 (2C, CO), 154.2 (8C, **L_3**), 152.2 (8C, **L_3**), 133.5 (8C, anthracene), 132.8 (4C, anthracene), 129.1 (4C, anthracene), 127.0 (8C, anthracene), 123.3 (4C, anthracene), 122.1 (4C, ethynyl), 119.4 (4C, **L_3**), 87.4 (4C, ethynyl), 15.9 (24C, PEt_3), 9.0 (24C, PEt_3). ^{31}P NMR ($CDCl_3$): δ 14.98 and 13.91.

2d. Complex **1a** (12.1 mg, 0.01 mmol) and N,N′-bis(4-pyridylidene)ethylenediamine (**L_4**; 2.4 mg, 0.01 mmol) were reacted in acetone to obtain **2d** in 94% yield. Anal. calcd (found) for $C_{112}H_{164}N_{12}O_{12}P_8Pt_4$: C, 46.40 (46.24); H, 5.70 (5.78); N, 5.79 (5.65). ESI-MS (*m*/*z*): 1387.00 [**2d** − $2NO_3^-$]$^{2+}$, 1269.14 [**2d** − $2NO_3^-$ − $2PEt_3$]$^{2+}$, 905.00 [**2d** − $3NO_3^-$]$^{3+}$, 786.20 [**2d** − $3NO_3^-$ − $3PEt_3$]$^{3+}$. IR data (KBr pellet, ν_{max}/cm^{-1}) for **2a**: 2105 (C≡C), 1600 (C═N). ^{1}H NMR (CD_3OD, 400 MHz): δ 9.22 (s, 2H, anthracene-H), 8.9 (d, 8H, pyridine-H), 8.5 (s, 4H, ═CH), 8.48 (s, 2H, anthracene-H), 8.09 (d, 4H, anthracene-H), 7.92 (d, 8H, pyridine-H), 7.5 (d, 4H, anthracene-H), 7.4 (m, 4H, anthracene-H), 4.2 (s, 8H, CH_2), 1.93 (q, 48H, PCH_2), 1.2 (t, 72H, PCH_3). ^{13}C NMR (CH_3NO_2 + $CDCl_3$): δ 154.4 (8C, **L_4**), 152.1 (8C, **L_4**), 133.5 (8C, anthracene), 132.8 (4C, anthracene), 128.3 (4C, anthracene), 127.0 (8C, anthracene), 123.2 (4C, anthracene), 122.2 (4C, ethynyl), 119.6 (4C, **L_4**), 111.5 (4C, **L_4**), 87.4 (4C, ethynyl), 61.0 (4C, **L_4**), 15.9 (24C, PEt_3), 9.0 (24C, PEt_3). ^{31}P NMR (CD_3OD): δ 14.42 (s, $^1J_{Pt-P}$ = 2872 Hz).

Acknowledgment. Financial support from the Council of Scientific and Industrial Research, New Delhi, India, is gratefully acknowledged. The authors are thankful to the reviewers for their fruitful comments and suggestions.

Supporting Information Available: CIF file giving X-ray data for **1a** and NMR and mass spectra. These materials are available free of charge via the Internet at http://pubs.acs.org.

IC801381P